Hydrodynamics of a DNA molecule in a flow field

R. G. Larson
Bell Laboratories, Lucent Technologies, 700 Mountain Avenue, Murray Hill, New Jersey 07974

T. T. Perkins, D. E. Smith, and S. Chu
Department of Physics, Stanford University, Stanford, California 94305

(Received 5 April 1996; revised manuscript received 19 August 1996)

The hydrodynamics of a single, fluorescing, DNA molecule held at one end by ''optical tweezers'' and subjected to a uniform flow are compared with Monte Carlo simulations that account for the molecule's entropic elasticity, Brownian motion, and hydrodynamic drag. Using self-diffusion data and analytic expressions to obtain the drag in the limits of the undeformed coil and of the fully stretched thread, the predicted chain stretching and mass distribution are in quantitative agreement with measurements. The results explain the success of the nonlinear elastic ''dumbbell'' model in predicting the rheological properties of dilute polymer solutions. [S1063-651X(97)00602-8]

PACS number(s): 87.15.He, 83.10.Nn, 83.20.Di, 83.20.Jp

The behavior of dilute flexible polymer molecules in flow remains controversial, despite a long history of experimental and theoretical study. The simplest theory, introduced by Kuhn [1] some 60 years ago, treats the polymer as an elastic ''dumbbell'' in which a ''spring'' connects two ''beads'' onto which are lumped the viscous drag forces that in reality act along the entire chain. Surprisingly, a finitely extensible dumbbell model is remarkably successful at predicting qualitatively the steady-state stresses and birefringence in flowing dilute polymer solutions [2]. However, light-scattering experiments [3] and more sophisticated theories [4] have called the predictions of this simple dumbbell model into question. Which refinements in the simple theory are really needed is still a matter of debate.

Recently we showed that the flow-induced deformation of a *single* flexible polymer could be directly studied by fluorescence microscopy of a DNA molecule tethered at one end to a small (~ 1 μm) microsphere held by optical tweezers in a uniform-velocity flow [5,6]. We found that plots of the fractional chain extension versus flow velocity V under flow scales as VL^m with $m=0.54\pm0.05$, for chains of length $20<L<80$ μm, suggesting that there is little or no change in the hydrodynamic interactions even when the DNA molecules are nearly fully extended.

In this paper we show using a self-consistent hydrodynamic model of DNA with no free parameters that this puzzling result is due to the limited length of the DNA molecules in the earlier study. Before describing the model, we therefore present additional data on longer chains, up to $L\approx150$ μm, and find that for $44<L<150$ μm [7], the apparent exponent increases to 0.75 ± 0.02; see the inset to Fig. 1. This change in power law was anticipated by Marko and Siggia [8].

The main body of Fig. 1 plots the measured relative extension x/L versus reduced velocity V/D for representative DNA molecules of contour length 44, 89, and 151 μm; x is the extension of the molecule, V is the velocity, and D is the measured center-of-mass diffusivity [9]. D is related to the translational drag coefficient, $\zeta_{\rm coil}k_BT$, of the undeformed molecules by the fluctuation-dissipation theorem, $\zeta_{\rm coil}=1/D$. With this scaling, the extension versus length curve shows a modest, but distinct, increase in slope for $x/L>0.3$ as the chain length increases.

Figure 2 shows the average distribution of DNA mass as a function of distance downstream from the tethering point for various flow velocities for a chain of length $L=67.2$ μm. These data were obtained by measuring the time-averaged fluorescence intensity distribution [6]. Note that the mass is most concentrated near the free end of the molecule where the tension is the least.

According to molecular theory, the steady-state deformation of the molecule is governed by the balance of the drag force against the entropic elastic force. The elastic properties of DNA in an aqueous solution obey the *wormlike chain* model; when the force (F) is applied to the free end of the chain, the equilibrium distance (r) separating the ends of the molecule is given by [10]

$$\frac{F(r)A}{k_BT}=\frac{1}{4}\left(1-\frac{r}{L}\right)^{-2}-\frac{1}{4}+\frac{r}{L}. \qquad (1)$$

Bustamante *et al.* [10] found that for their unlabeled DNA molecules, the presistence length is $A\approx0.053$ μm. Diffusion-coefficient data of the labeled DNA [9] compared to unlabeled DNA [11] suggest that A may be slightly larger because of dye intercalation. Charges on the DNA molecule might also affect A, but should produce no further complications since for the electrolyte used the Debye length is estimated to be only around 10 nm. Finally, Eq. (1) fails when the tension F approaches the value of around 70 pN required to ''overstretch'' a DNA molecule [12,13]. From the simulations described below, we find that at the tethering point the tension reaches its maximum value of 5 pN, at the highest reduced velocity V/D of 500 μm^{-1}. Thus along the entire contour of the DNA molecule the tension is well within the range for which Eq. (1) applies.

In the dumbbell model, the drag forces are lumped onto the ''beads'' at the two free ends of the molecule. For the tethered chain, there is only one free end at which to apply the drag force; thus the appropriate simple model is a ''half

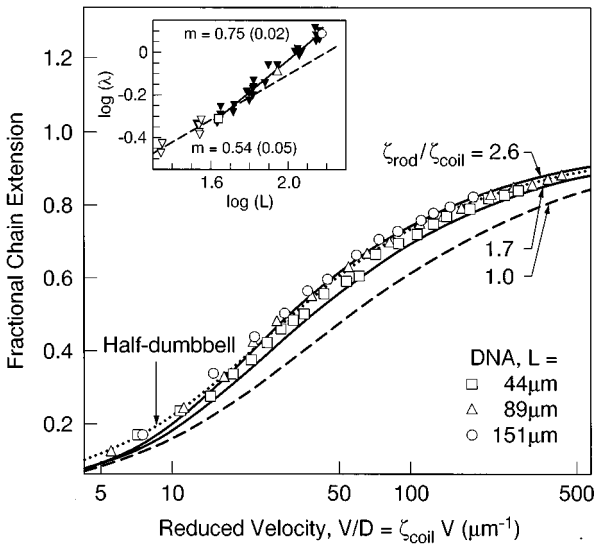

FIG. 1. The inset shows the shift factor λ by which the velocity V must be multiplied to superpose curves of fractional chain extension versus V for various DNA chain lengths L. Data for the ranges $L \geqslant 40$ μm (▼,□,△,○) and $L \leqslant 80$ μm are fitted separately by $\lambda \propto L^m$, yielding $m=0.75$ for the former range and $m=0.54$ for the latter. The main plot contains the ''best representative'' data sets corresponding to the three open symbols (□,△,○) closest to the solid line in the inset; D is the diffusivity. The dotted line is the prediction of the ''half-dumbbell model,'' i.e., it is the force-extension curve for the wormlike chain with a reduced force F/k_BT equal to $0.73\zeta_{\text{coil}}V$ applied to the chain end. The solid lines are the predictions of the simulation for values of the hydrodynamic interaction parameter $h=1.3$ and 4.0, corresponding to $\zeta_{\text{rod}}/\zeta_{\text{coil}}=1.7$ and 2.6, respectively, for chain lengths of 44 and 151 μm. The dashed line is the prediction for a hypothetical molecule with $h=0$; i.e., $\zeta_{\text{rod}}/\zeta_{\text{coil}}=1$, and no change in hydrodynamic drag due to molecular stretching.

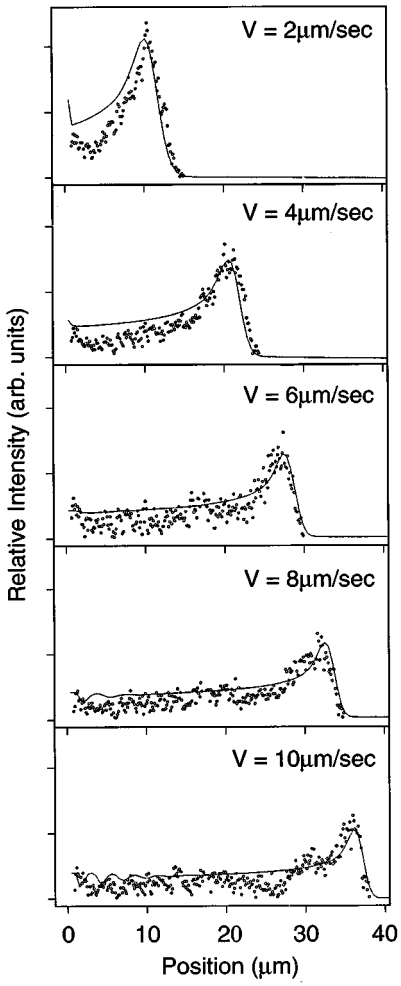

FIG. 2. Computed distribution of bead mass as a function of position downstream of the tether point for $N=80$ and $L=67.2$ μm at the values of V shown (lines), compared to the measured distribution of DNA mass for $L=67.2$ μm (symbols), replotted from Ref. [6]. The value of the parameter $\zeta_{\text{coil}}=4.8$ sec$(\mu\text{m})^{-2}$ is obtained from the diffusivity measurements of Smith, Perkins, and Chu [9], and $h=1.5$ is chosen so that the ratio $\zeta_{\text{rod}}/\zeta_{\text{coil}}=1.9$ agrees with the theoretical estimates from Eqs. (5) and (6). The simulated distributions were obtained by counting repeatedly ($\sim 10^5$ times) the number of beads in bins of width 0.5 μm, and averaging together the results. A small binning artifact produces the oscillations at large V and small positions.

dumbbell,'' with the spring force given by Eq. (1). This model gives the prediction shown by the dotted line in Fig. 1. Clearly, the curve of deformation versus velocity is extremely well matched by the dumbbell model, although a quantitative fit requires setting the drag coefficient of the ''bead'' on the half dumbbell equal to 0.73 times the measured drag coefficient $\zeta_{\text{coil}}k_BT=1/D$ of the undeformed coil. This 27% reduction can be understood qualitatively by noting that a smaller drag force applied entirely at the chain end can produce the same degree of stretching as a larger force that is distributed along the entire contour of the chain.

To understand why such a naive model works so well, we consider a more complete model in which the drag force is distributed nearly continuously along the chain contour, and increases in magnitude as the chain is deformed. We use a ''coarse grained'' representation in which the drag force is distributed onto a sequence of beads connected together by short submolecules. The fully extended length of each submolecule is $l=L/N$, where N is the number of beads. Essentially identical results are obtained for $N=40$ or 80 [7]. The elastic ''spring'' force F_i^s for each submolecule is obtained from Eq. (1) by replacing L with the length of the submolecule l:

$$\frac{F_i^s A_{\text{eff}}}{k_BT}=\frac{1}{4}\left(1-\frac{r_i}{l}\right)^{-2}-\frac{1}{4}+\frac{r_i}{l}, \tag{2}$$

where r_i is the separation distance between bead $i-1$ and bead i. The introduction of beads into the wormlike chain slightly increases its flexibility, because the beads act like free hinges which do not transmit a bending moment. This effect is small because the chain's persistence length is small compared to the spacing of the beads along the contour of the chain, and can be canceled out merely by modestly increasing the persistence length A_{eff} of the subchain. By applying in the simulations a fixed force to the end of the chain, and computing the resulting average chain extension, the known elastic properties of DNA of length 67 μm, for example, are reproduced by the model with 40 beads when $A_{\text{eff}}=0.061$ μm [7].

To account for variations in the hydrodynamic drag coefficients that occur when the macromolecule is stretched out

in the flow, we use the average separations between beads to compute the effective hydrodynamic interactions between them. The average distance downstream of the tether point of bead i, $\langle x_i \rangle$, and corresponding drag coefficient ζ_i are then calculated self-consistently. Fluctuations in hydrodynamic interactions are neglected.

Using the Oseen theory to describe the hydrodynamic interactions between each pair of beads [14], the drag force on bead i is given by

$$F_i^d = V\zeta kT - \frac{h}{N}\sum_{j\neq i}\Omega_{ij}F_j^d, \tag{3}$$

where V is the flow velocity, ζ is the ''bare'' drag coefficient for a single bead without hydrodynamic interactions with other beads, and Ω_{ij} is the Oseen coefficient that accounts for the hydrodynamic interaction between beads i and j; it depends inversely on the average separation between beads i and j. To keep Ω_{ij} from diverging, we introduce a cutoff length R, where $R \equiv \sqrt{2AL}$ is roughly the root-mean-square separation of the chain ends at zero flow:

$$\Omega_{ij} \equiv \begin{cases} 1, & |\langle x_i \rangle - \langle x_j \rangle| \leqslant R \\ R/|\langle x_i \rangle - \langle x_j \rangle|, & |\langle x_i \rangle - \langle x_j \rangle| \geqslant R. \end{cases} \tag{4}$$

Variations in drag begin to occur when the average extension of the molecule exceeds R. The effects of varying this cutoff length over the range $R/2$ to $2R$ were investigated and found to be smaller than experimental error. The coefficient h in Eq. (3) is a dimensionless prefactor that sets the scale of the changes in hydrodynamic drag that occur as the chain is extended. It can be obtained from the ratio of the drag coefficient for the fully extended molecule $\zeta_{\rm rod}k_BT$ to that of the undistorted coil $\zeta_{\rm coil}k_BT$. These drag coefficients are [15]

$$\zeta_{\rm coil}k_BT = \frac{3}{8}(6\pi^3)^{1/2}\eta_s R = 5.11R\eta_s = \frac{k_BT}{D} \tag{5}$$

and

$$\zeta_{\rm rod}k_BT = \frac{2\pi L\eta_s}{\ln(L/d)} = \frac{6.28L\eta_s}{\ln(L/d)}, \tag{6}$$

where $d \approx 2$ nm is the diameter of a DNA molecule [11,16].

Using the measured dependence of $D = 1/\zeta_{\rm coil}$ on L for DNA molecules with lengths in the range $L = 22$–140 μm, and Eq. (6), one finds that $\zeta_{\rm rod}/\zeta_{\rm coil}$ is surprisingly small; it increases from 1.7 to 2.6 as L increases from 22 to 151 μm. The main reason for this small ratio is the presence of the logarithmic dividing factor, $\ln(L/d) = 9$–11 in Eq. (6), which is rather large because of DNA's enormous aspect ratio $L/d = 10\,000$–$75\,000$ [17]. The parameters ζ and h in Eq. (3) can be obtained by requiring that the predicted drag coefficient for the whole chain, $(\Sigma_i F_i^d)/V$, be equal to $\zeta_{\rm coil}k_BT$ for the undeformed chain, and be equal to $\zeta_{\rm rod}k_BT$ for the completely extended chain. We find that an increase in $\zeta_{\rm rod}/\zeta_{\rm coil}$ from 1.7 to 2.6 corresponds to an increase in h from 1.3 to 4.0.

For each bead in a uniform flow, the sum of the spring and the drag forces can be expressed as the gradient of a *bead potential* W_1:

$$\mathbf{F}_i = \mathbf{F}_i^s + \mathbf{F}_{i+1}^s + \mathbf{F}_i^d = \boldsymbol{\nabla}_i W_i, \tag{7}$$

where $\mathbf{F}_i^s$ is the spring force acting between bead i and bead $i-1$, and

$$\frac{W_i}{k_BT} \equiv \frac{l}{A}\sum_{j=0}^{j=1}\left\{\frac{1}{4}\left(1-\frac{r_{i+j}}{l}\right)^{-1} - \frac{1}{4}\left(\frac{r_{i+j}}{l}\right) + \frac{1}{2}\left(\frac{r_{i+j}}{l}\right)^2\right\} - x_i\zeta_i V, \tag{8}$$

where $\zeta_i \equiv F_i^d/(Vk_BT)$ is an effective drag coefficient that accounts for hydrodynamic interactions among the beads.

With this potential, steady-state configuration distributions incorporating Brownian motion are calculated using a standard Metropolis Monte Carlo scheme, and accurate averages are obtained using about $10^4 \times N^3$ moves per run. The model calculations involve *no adjustable parameters*.

The solid lines in Fig. 1 show the predicted extension for 44- and 151-μm-long DNA molecules, corresponding to $\zeta_{\rm rod}/\zeta_{\rm coil} = 1.7$ and 2.6. These calculations are nearly in agreement with the DNA data and with the dumbbell model.

The comparison in Fig. 1 reveals why the dumbbell model works so well. Consider the dumbbell model as the zero-order description. The first correction is to distribute the drag along the length of the polymer, which gives the $\zeta_{\rm rod}/\zeta_{\rm coil} = 1$ curve in Fig. 1; this ''improvement'' in the theory leads to a deviation from the data. A second correction is to include the dependence of the drag coefficient on the extension; this gives the curves for $\zeta_{\rm rod}/\zeta_{\rm coil} = 1.7$ and 2.6, which restore agreement with the data, and with the simple dumbbell model. Thus, by neglecting both the distribution of drag along the chain and the deformation dependence of the drag coefficient, the dumbbell model makes two errors that largely cancel each other out, at least for the molecular lengths considered here. A similar fortuitous cancellation of errors can be expected for typical synthetic polymers (such as polystyrene) of roughly 10^5–10^6 Daltons.

The lines in Fig. 2 show the computed average distribution of bead mass versus distance downstream from the tethering point for $L = 67.2$ μm. The appropriate value of $\zeta_{\rm rod}/\zeta_{\rm coil}$ for this chain length is around 1.9. The agreement between experimental and simulated mass density is generally very good [18].

In summary, then, the surprising accuracy of the dumbbell model in describing the shape of the steady-state velocity-extension curve is due in part to a cancellation of effects: the distribution of drag forces along the chain modestly reduces the slope of fractional extension versus velocity, while the increase in effective drag coefficient with chain extension modestly steepens it. For DNA molecules of $L \approx 40$–150 μm, these two effects largely cancel out, and the steepness of the velocity-extension curve is close to that of a simple nonlinear dumbbell with no deformation dependence of the drag coefficient. The accuracy of the dumbbell model is enhanced by the mass distribution, with its high concentration of monomer, and hence of drag force, near the chain end [19]. Thus experimental studies of the hydrodynamics of single DNA molecules in a simple flow conform to the classical picture of the dynamics and rheology of flexible polymer molecules,

in which three forces—the elastic spring force, hydrodynamic drag with a nearly constant drag coefficient, and the Brownian force—provide a complete physical model, at least at steady state. These results help explain the success of the dumbbell model in predicting rheological data of dilute solutions of flexible polymers, and suggest that the inclusion of any ''new'' physics into the theory of the dilute-solution flow behavior of polymer molecules is unwarranted.

[1] W. Kuhn, Kolloid Z. **68**, 2 (1934).

[2] G. G. Fuller and L. G. Leal, Rheol. Acta **19**, 580 (1980); P. N. Dunlap and L. G. Leal, J. Non-Newt. Fluid Mech. **23**, 5 (1987); V. Tirtaatmadja and T. Sridhar, J. Rheol. **39**, 1133 (1995).

[3] F. R. Cottrell, E. Q. Merrill, and K. A. Smith, J. Polym. Sci. Part A-2 **27**, 1415 (1969); R. C. Armstrong, S. K. Gupta, and O. Basaran, Polym. Eng. Sci. **20**, 466 (1980); M. J. Menasveta and D. A. Hoagland, Macromolecules **24**, 3427 (1991).

[4] A. Peterlin, Pure Appl. Chem. **12**, 563 (1966); M. Fixman, J. Chem. Phys. **45**, 785 (1966); **45**, 793 (1966); P. G. de Gennes, *ibid.* **60**, 5030 (1974); E. J. Hinch, in *Proceedings Internationaux Centre de la Recherche Scientifique* (Editions du Centre National de la Recherche Scientifique, Paris, 1974), No. 233, p. 241; R. J. Cerf, Adv. Polym. Phys. **1**, 382 d(1959); G. G. Fuller and L. G. Leal, J. Non-Newt. Fluid Mech. **8**, 271 (1981); D. H. King and D. F. James, J. Chem. Phys. **78**, 4749 (1983).

[5] T. T. Perkins, D. E. Smith, and S. Chu, Science **264**, 819 (1994).

[6] T. T. Perkins, D. E. Smith, R. G. Larson, and S. Chu, Science **268**, 83 (1995).

[7] R. G. Larson, T. T. Perkins, D. E. Smith, and S. Chu (unpublished).

[8] J. F. Marko and E. D. Siggia, Macromolecules **28**, 8759 (1995).

[9] D. E. Smith, T. T. Perkins, and S. Chu, Macromolecules **29**, 1372 (1996).

[10] C. Bustamante, J. F. Marko, E. D. Siggia, and S. Smith, Science **265**, 1599 (1994); A. Vologodskii, Macromolecules **27**, 5623 (1994).

[11] R. Pecora, Science **251**, 893 (1991).

[12] P. Cluzel, A. Lebrun, C. Heller, R. Lavery, J.-L. Viovy, D. Chatenay, and F. Caron, Science **271**, 792 (1996).

[13] S. B. Smith, Y. Cui, and C. Bustamante, Science **271**, 795 (1996).

[14] R. B. Bird, C. F. Curtiss, R. C. Armstrong, and O. Hassager, *Dynamics of Polymeric Liquids*, 2nd ed. (Wiley, New York, 1987), Vol. 2.

[15] M. Doi and S. F. Edwards, *The Theory of Polymer Dynamics* (Oxford, New York, 1986).

[16] W. Eimer and R. Pecora, J. Chem. Phys. **94**, 2324 (1991).

[17] Equation (6) neglects any hydrodynamic effect of the glass surfaces that are 15 μm above and 60 μm below the DNA chain. The effect of these moving no-slip surfaces is equivalent to that of stationary ''image'' DNA molecules $\xi_t = 30$ μm above and $\xi_b = 120$ μm below the real DNA molecule. As an upper bound for the effect of these ''image'' molecules, we replace the surfaces by a moving cylindrical tube with radius $\xi/2$ with the DNA along its axis, with $\xi = \xi_t$. For large L/ξ, this changes the log term in Eq. (6) to $\ln(\xi/d)$, and increases $\zeta_{\rm rod}$ by at most 16% for $L = 151$ μm. See G. K. Batchelor, J. Fluid Mech. **46**, 813 (1971). The actual correction is likely to be much less than this.

[18] Although there appears to be an overprediction of the average mass density of the most highly stretched DNA near the tether point, the measured mass density in this region at $V \geqslant 4$ μm/sec is on average actually less than that corresponding to 100% stretching. In light of our force estimates showing the tension to be much less than that required for overstretching, the most likely source of this disagreement is experimental error due to a possible overestimation of background light intensity (which was subtracted from the data in Fig. 2), or systematic measurement error due to the very faint intensity of light radiating from the most highly stretched portion of the molecule.

[19] J. Frenkel, Acta Physicochim. URSS **19**, 51 (1944); G. Ryskin, J. Fluid Mech. **178**, 423 (1987).